

CERN-EP-2024-215
09 August 2024

First determination of the spin-parity of $\Xi_c(3055)^{+,0}$ baryons

LHCb collaboration[†]

Abstract

The $\Xi_b^{0(-)} \rightarrow \Xi_c(3055)^{+(0)} (\rightarrow D^{+(0)} \Lambda) \pi^-$ decay chains are observed, and the spin-parity of $\Xi_c(3055)^{+(0)}$ baryons is determined for the first time. The measurement is performed using proton-proton collision data at a center-of-mass energy of $\sqrt{s} = 13$ TeV, corresponding to an integrated luminosity of 5.4 fb^{-1} , recorded by the LHCb experiment between 2016 and 2018. The spin-parity of the $\Xi_c(3055)^{+(0)}$ baryons is determined to be $3/2^+$ with a significance of more than 6.5σ (3.5σ) compared to all other tested hypotheses. The up-down asymmetries of the $\Xi_b^{0(-)} \rightarrow \Xi_c(3055)^{+(0)} \pi^-$ transitions are measured to be $-0.92 \pm 0.10 \pm 0.05$ ($-0.92 \pm 0.16 \pm 0.22$), consistent with maximal parity violation, where the first uncertainty is statistical and the second is systematic. These results support the hypothesis that the $\Xi_c(3055)^{+(0)}$ baryons correspond to the first D -wave λ -mode excitation of the Ξ_c flavor triplet.

Submitted to Phys. Rev. Lett.

© 2024 CERN for the benefit of the LHCb collaboration. [CC BY 4.0 licence](https://creativecommons.org/licenses/by/4.0/).

[†]Authors are listed at the end of this paper.

Baryons containing a single heavy quark, hereafter referred to as singly heavy baryons, provide an ideal laboratory for studying the complex quark dynamics. Their structures can be effectively described by the approximation of a heavy quark and a diquark system of light quarks, with the dynamics primarily governed by the diquark degrees of freedom [1]. Based on the spin-flavor wave function of the diquark, the ground states can be categorized into flavor antisymmetrical triplets, denoted as $\bar{3}_F$, and flavor symmetrical sextuplets denoted as 6_F , respectively [2]. Excitation can occur either between the two light quarks, known as the ρ mode, or between the heavy quark and the diquark, referred to as the λ mode. Considering the various excitation modes and spin-angular momentum configurations, a rich spectrum of singly-heavy baryons is expected, providing insights into the confinement mechanism of the strong interaction [3].

Numerous excited singly charmed baryons have been observed by Belle [4–11], BaBar [12–14], and LHCb [15–17] experiments in the last two decades. While many theoretically allowed states remain undiscovered, most of the observed resonances, including the $\Xi_c(3055)^{+(0)}$ baryons, have not yet been well established in terms of their excitation nature. The $\Xi_c(3055)^+$ baryon, with quark content csu , was observed in the $\Sigma_c^{++}K^-$ and $D^+\Lambda$ final states [9, 10, 14].¹ Its isospin partner, the $\Xi_c(3055)^0$ baryon with quark content csd , was observed in the $D^0\Lambda$ final state [10]. A number of possible explanations for the excitation modes have been proposed based on their masses, widths, and strong decay properties. In Refs. [18–27], the $\Xi_c(3055)^{+(0)}$ states are interpreted as the D -wave orbital angular momentum excitation with possible spin-parity (J^P) assignments of $3/2^+$, $5/2^+$ or $7/2^+$. The second orbital excitation of the λ mode is favored over the ρ mode or a combination of both [20, 25]. The strong decays of the $\Xi_c(3055)^+$ state to the $\Sigma_c^{++}K^-$ and $D^+\Lambda$ final states, studied in the 3P_0 model, suggest that it may be a $2S$ excitation of the $\Xi_c(3_F)$ or $\Xi'_c(6_F)$ state, with $J^P = 1/2^+$ or $3/2^+$ [26]. Hadron molecular states have also been proposed [28] to interpret the $\Xi_c(3055)^{+(0)}$ baryons, with $J^P = 1/2^-$ or $3/2^-$. Thus, measurements of the spin-parity of the $\Xi_c(3055)^{+(0)}$ baryons are crucial to pin down their nature and clarify the complicated charm-baryon spectrum.

The spin-parity of the $\Xi_c(3055)^{+(0)}$ baryons can be studied by exploiting the weak decays $\Xi_b^{0(-)} \rightarrow \Xi_c(3055)^{+(0)}\pi^-$. In this work, amplitude analyses of $\Xi_b^{0(-)} \rightarrow \Xi_c^{**+(0)}\pi^-$ decays are performed, where the $\Xi_c^{**+(0)}$ states refer to excited $\Xi_c(3055)^{+(0)}$ or $\Xi_c(3080)^{+(0)}$ baryons and are reconstructed in the $D^{+(0)}\Lambda$ final states. The spin-parity, masses and widths of the $\Xi_c(3055)^{+(0)}$ baryons are determined, as well as the up-down asymmetries of the $\Xi_b^{0(-)} \rightarrow \Xi_c(3055)^{+(0)}\pi^-$ transitions, which are defined as the relative difference between the decay rates for the up and down helicity states [29] of the $\Xi_b^{0(-)}$ baryons. The analysis is performed using proton-proton (pp) collision data at a center-of-mass energy of $\sqrt{s} = 13$ TeV, corresponding to an integrated luminosity of about 5.4 fb^{-1} , collected with the LHCb detector between 2016 and 2018.

The LHCb detector, designed for the study of particles containing b or c quarks, is a single-arm forward spectrometer covering the pseudorapidity range $2 < \eta < 5$, described in detail in Refs. [30, 31]. The online event selection for Ξ_b decays is performed by a trigger [32] which consists of a hardware stage followed by a two-step software stage [33–36]. The hardware trigger decision is based on either the transverse energy (the energy component perpendicular to the beam direction) deposited in the hadronic calorimeter by a particle associated with the signal decay, or on signatures from other collision products. The

¹The inclusion of charge-conjugated processes is implied throughout.

first step of the software trigger requires a single track or a pair of tracks with sufficient transverse momentum and impact parameter, which is defined as the minimum distance of the track relative to the primary pp interaction vertex (PV). In the second step, the presence of a secondary vertex that is well separated from the PV is required.

Simulated samples are used to optimize the selection criteria, parameterize the invariant-mass distributions and characterize the detector resolution and efficiencies. These samples are generated using the software described in Refs. [37–42]. In the simulation, the products of the $\Xi_b^{0(-)}$, $\Xi_c^{*+ (0)}$, $D^{+(0)}$ and Λ decays are generated uniformly over the allowed phase space. The properties of partially reconstructed $\Xi_b^{0(-)}$ decays are modelled with a fast parametric simulation [43].

In the offline reconstruction, charged tracks identified as protons, kaons or pions are combined to form $\Lambda \rightarrow p\pi^-$, $D^+ \rightarrow K^-\pi^+\pi^+$ and $D^0 \rightarrow K^-\pi^-$ candidate decays. The reconstructed Λ , D^+ and D^0 vertices are required to have good quality and be significantly displaced from any PV. The invariant masses of $D^{+(0)}$ and Λ candidates are required to be within $\pm 20 \text{ MeV}/c^2$ and $\pm 6 \text{ MeV}/c^2$ of the known values [44], respectively. The $D^{+(0)}$ and Λ candidates are combined with an additional π^- track to form $\Xi_b^{0(-)}$ candidates. To improve the resolution of the reconstructed $\Xi_b^{0(-)}$ invariant mass, denoted as $m_{D^{+(0)}\Lambda\pi^-}$, a kinematic fit is applied [45], constraining the $D^{+(0)}$ and Λ invariant masses to their known values and imposing the $\Xi_b^{0(-)}$ momentum to point back to the associated PV. The multi-layer perceptron (MLP) neural network implemented in the TMVA toolkit [46] is utilized to further distinguish the $\Xi_b^{0(-)}$ signal from the combinatorial background. An MLP classifier is trained for Ξ_b^0 and Ξ_b^- decays independently, which combines the kinematic and vertexing information of the $\Xi_b^{0(-)}$ baryon and its decay products.

Extended maximum-likelihood fits are performed to the $m_{D^{+(0)}\Lambda\pi^-}$ distributions to determine the signal yields. The $\Xi_b^{0(-)}$ signal components are described by the combination of a Gaussian function and a double-sided Crystal Ball function [47]. The background due to $\Xi_b^{0(-)} \rightarrow D^{+(0)}\Sigma^0(\rightarrow \Lambda\gamma)\pi^-$ decays, with the photon not reconstructed, is modelled using fast simulation [43]. The combinatorial background is described by an exponential function. The yields of the signal and these two background components are allowed to vary in the fits. The $m_{D^{+(0)}\Lambda\pi^-}$ distributions and fit results are shown in Fig. 1. The total $\Xi_b^{0(-)}$ yields are measured to be 637 ± 31 (232 ± 19). The *sPlot* technique [48] is used to assign a weight to each $\Xi_b^{0(-)}$ candidate based on the fit results to subtract the background.

The polarization of Λ_b^0 baryons at the LHC has been measured to be consistent with zero [49]. Assuming the $\Xi_b^{0(-)}$ baryons are also produced unpolarized, the $\Xi_b^{0(-)} \rightarrow D^{+(0)}\Lambda\pi^-$ decay kinematics are fully described by the invariant mass $m_{D^{+(0)}\Lambda}$ and three angular variables $\vec{\Omega} \equiv (\cos\theta_{\Xi_c^{+(0)}}, \phi_\Lambda, \cos\beta_\Lambda)$. The variable $\theta_{\Xi_c^{+(0)}}$ is the angle between the Λ momentum and the momentum of the pion from the $\Xi_b^{0(-)}$ decay, in the rest frame of the $D^{+(0)}\Lambda$ system (denoted as $\Xi_c^{+(0)}$), and is referred to as the $\Xi_c^{+(0)}$ helicity angle. Similarly, the Λ helicity angle β_Λ is defined by the momentum of the proton and that of the $D^{+(0)}$ meson in the Λ rest frame. The variable ϕ_Λ is the angle between the $\Xi_c^{+(0)} \rightarrow D^{+(0)}\Lambda$ and $\Lambda \rightarrow p\pi^-$ decay planes. These angles are illustrated in Fig. 5 in Appendix 1. The distributions of these variables are shown in Figs. 2 and 3 for the Ξ_b^0 and Ξ_b^- channels, respectively, where the background is subtracted using the *sPlot* weights. The $D^{+(0)}\Lambda$ invariant-mass spectra clearly exhibit the $\Xi_c(3055)^{+(0)}$ resonances, and also

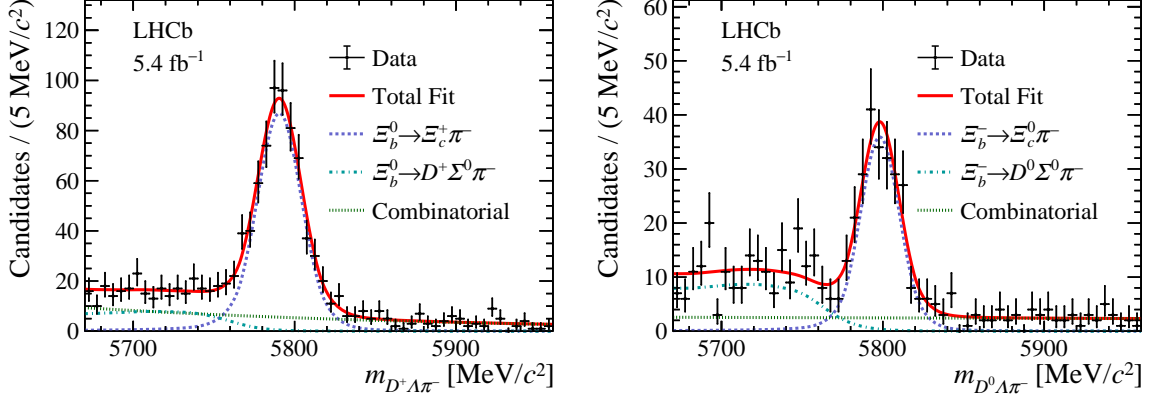


Figure 1: Distributions of the (left) $D^+\Lambda\pi^-$ and (right) $D^0\Lambda\pi^-$ invariant mass with the fit results overlaid.

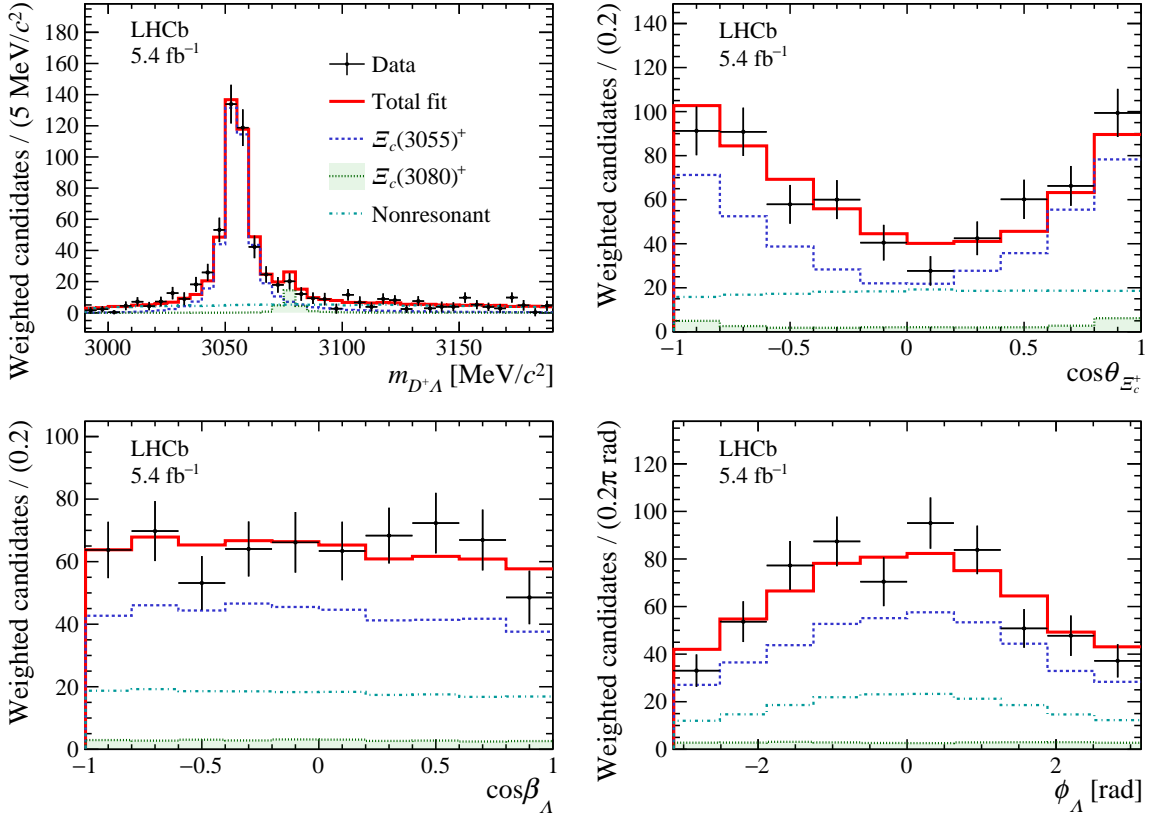


Figure 2: Distributions of the (top left) $D^+\Lambda$ invariant mass, (top right) Ξ_c^+ helicity angle, (bottom left) Λ helicity angle and (bottom right) azimuthal angle, for the $\Xi_b^0 \rightarrow D^+\Lambda\pi^-$ sample. The projections of the amplitude fit under the spin-parity hypothesis $J_{\Xi_c(3055)^+}^P = 3/2^+$ are overlaid.

hint at the presence of the $\Xi_c(3080)^{+(0)}$ state as well as a nonresonant (NR) contribution. This is the first observation of the $\Xi_c(3055)^{+(0)}$ baryons in $\Xi_b^{0(-)}$ decays.

Amplitude analyses for the Ξ_b^0 and Ξ_b^- channels are carried out separately. In the following description, the notation applies to the Ξ_b^0 channel, but is similar for the Ξ_b^-

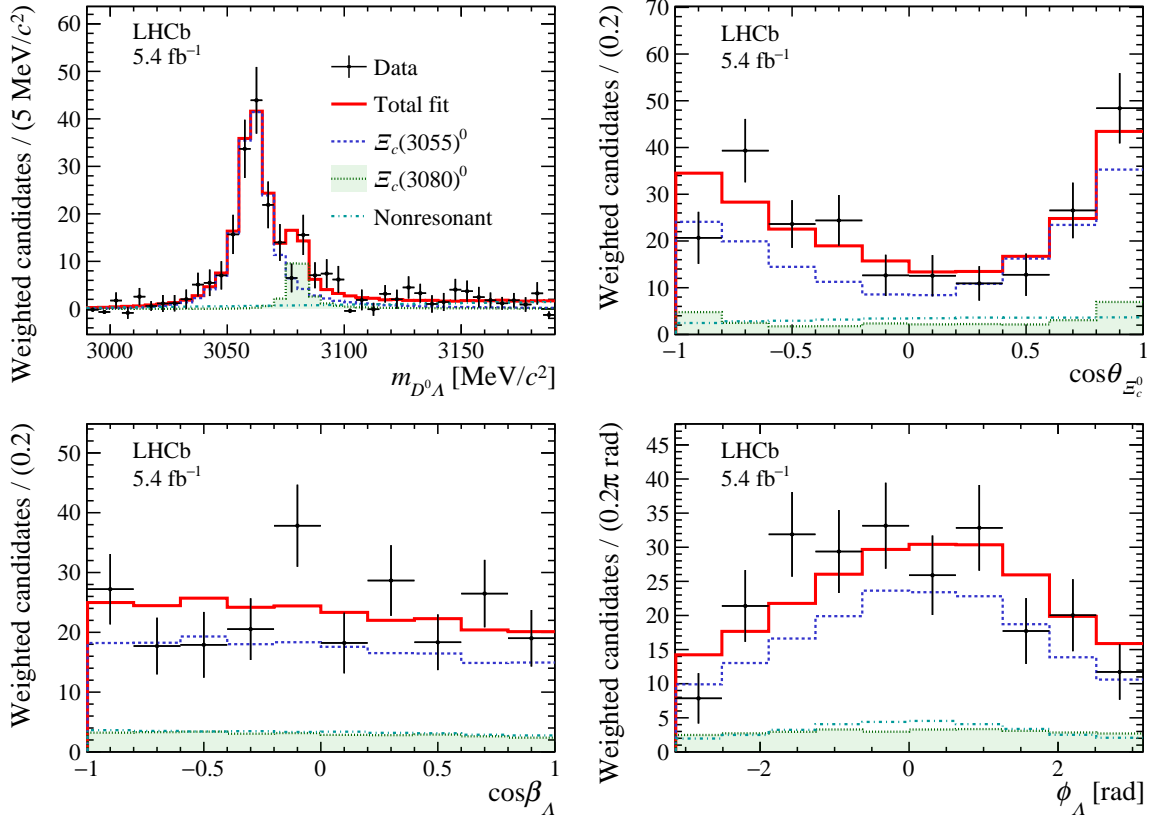


Figure 3: Distributions of the (top left) $D^0\Lambda$ invariant mass, (top right) Ξ_c^0 helicity angle, (bottom left) Λ helicity angle and (bottom right) azimuthal angle, for the $\Xi_b^- \rightarrow D^0\Lambda\pi^-$ sample. The projections of the amplitude fit under the spin-parity hypothesis $J_{\Xi_c(3055)^0}^P = 3/2^+$ are overlaid.

channel. An unbinned maximum-likelihood fit is performed to the four-dimensional $\Xi_b^0 \rightarrow D^+\Lambda\pi^-$ distribution using an amplitude model of the $m_{D+\Lambda}$ and $\vec{\Omega}$ observables. The fit model accounts for various J^P hypotheses: $J^P = 1/2^\pm, 3/2^\pm, 5/2^\pm$ or $7/2^\pm$ for the $\Xi_c(3055)^+$ baryon, $3/2^\pm$ or $5/2^\pm$ for the $\Xi_c(3080)^+$ baryon, and $1/2^\pm$ for the nonresonant component. The combination of the J^P hypotheses that gives the largest likelihood value is considered as the favored one. The logarithm of the likelihood function ($\log \mathcal{L}$) is defined as

$$\log \mathcal{L}(\vec{v}) = \frac{\sum_i w_i}{\sum_i w_i^2} \sum_i w_i \times \log \left[\mathcal{P}(m_{D+\Lambda}^i, \vec{\Omega}^i | \vec{v}) \right], \quad (1)$$

where $\mathcal{P}(m_{D+\Lambda}, \vec{\Omega} | \vec{v})$ is the signal probability density function (PDF), w_i is the signal *sPlot* weight [50], the index i runs over the Ξ_b^0 candidates in data, and \vec{v} denotes the vector of free parameters. The factor $\sum_i w_i / \sum_i w_i^2$ is applied for a correct determination of the fit parameter uncertainties [51] in the presence of background.

The PDF is formed by the the squared amplitude summed over the helicities of the

Ξ_b^0 baryon, $\lambda_{\Xi_b^0}$, and of the proton λ_p , as

$$\begin{aligned} \mathcal{P}(m_{D^+\Lambda}, \vec{\Omega}|\vec{\nu}) &= \frac{1}{I(\vec{\nu})} \sum_{\lambda_{\Xi_b^0}, \lambda_p} \left| \mathcal{M}_{\lambda_{\Xi_b^0}, \lambda_p}(m_{D^+\Lambda}, \vec{\Omega}|\vec{\nu}) \right|^2 \\ &\times \Phi(m_{D^+\Lambda}, \vec{\Omega}) \epsilon(m_{D^+\Lambda}, \vec{\Omega}), \end{aligned} \quad (2)$$

where $\Phi(m_{D^+\Lambda}, \vec{\Omega})$ is the phase-space density function that depends on the final state kinematics, and $\epsilon(m_{D^+\Lambda}, \vec{\Omega})$ is the experimental efficiency that is evaluated with simulation. The normalization is given by

$$\begin{aligned} I(\vec{\nu}) &\equiv \int \sum_{\lambda_{\Xi_b^0}, \lambda_p} \left| \mathcal{M}_{\lambda_{\Xi_b^0}, \lambda_p}(m_{D^+\Lambda}, \vec{\Omega}|\vec{\nu}) \right|^2 \\ &\times \Phi(m_{D^+\Lambda}, \vec{\Omega}) \epsilon(m_{D^+\Lambda}, \vec{\Omega}) dm_{D^+\Lambda} d\vec{\Omega}, \end{aligned} \quad (3)$$

and is calculated numerically with a Monte Carlo integration method [52] utilizing simulated $\Xi_b^0 \rightarrow D^+\Lambda\pi^-$ decays. The signal decay amplitude $\mathcal{M}_{\lambda_{\Xi_b^0}, \lambda_p}(m_{D^+\Lambda}, \vec{\Omega}|\vec{\nu})$ is constructed based on the helicity formalism [29], for which the full formula is described in detail in Appendix 1. In the amplitude model, the invariant-mass distributions of the $\Xi_c(3055)^+$ and $\Xi_c(3080)^+$ resonances are each described by a relativistic Breit–Wigner function [44], and that of the nonresonant component is described empirically by an exponential function. The mass and width of the $\Xi_c(3055)^+$ baryon are free parameters in the fit, while those of the $\Xi_c(3080)^+$ baryon are fixed to the known values [44]. The helicity couplings for each $\Xi_b^0 \rightarrow \Xi_c^+\pi^-$ decay, $H_{\lambda_{\Xi_b^0}}$, with $\lambda_{\Xi_b^0} = \pm 1/2$ are free to vary. They are used to define the up-down asymmetry of the decay as

$$\alpha \equiv \frac{|H_{\lambda_{\Xi_b^0}=+1/2}|^2 - |H_{\lambda_{\Xi_b^0}=-1/2}|^2}{|H_{\lambda_{\Xi_b^0}=+1/2}|^2 + |H_{\lambda_{\Xi_b^0}=-1/2}|^2}, \quad (4)$$

for which a nonzero value indicates parity symmetry violation [53]. The helicity couplings for the $\Lambda \rightarrow p\pi^-$ decay are fixed to the precise measurement obtained by BESIII [54].

Among all the considered spin-parity assignments, the combination of $J_{\Xi_c(3055)^+}^P = 3/2^+$, $J_{\Xi_c(3080)^+}^P = 5/2^+$, and $J_{\text{NR}}^P = 1/2^-$ gives the largest maximum likelihood. The projections of the corresponding amplitude model are overlaid with data distributions in Fig. 2. In this scenario, the $\Xi_c(3055)^+$ and $\Xi_c(3080)^+$ baryons are consistent with the two D -wave excitations of the Ξ_c^+ flavor triplet, where the charm quark spin is antiparallel or parallel to the orbital angular momentum, respectively. The nonresonant component is consistent with an S -wave decay to the $D^+\Lambda$ final state. The significance of the $\Xi_b^0 \rightarrow \Xi_c(3080)^+(\rightarrow D^+\Lambda)\pi^-$ signal is determined to be 4.4σ , with a likelihood-ratio test considering amplitude models with or without the $\Xi_c(3080)^+$ contribution. The branching fraction for the $\Xi_c(3080)^+$ baryon relative to that for the $\Xi_c(3055)^+$ baryon in the $\Xi_b^0 \rightarrow \Xi_c^{*++}(\rightarrow D^+\Lambda)\pi^-$ decay, denoted as R_B , is measured by comparing the integral of the PDF for the $\Xi_c(3080)^+$ component to that of the $\Xi_c(3055)^+$ baryon. The mass and width of the $\Xi_c(3055)^+$ baryon, and the up-down asymmetry of the $\Xi_b^0 \rightarrow \Xi_c(3055)^+\pi^-$ decay are also measured.

According to theoretical calculations for a $\bar{3}_F$ beauty baryon decaying to a $\bar{3}_F$ charm baryon and a pseudoscalar via a color-allowed process, where factorization is expected to

Table 1: Measurement of the masses (m) and widths (Γ) for the $\Xi_c(3055)^{+(0)}$ baryons, the up-down asymmetries (α) of the $\Xi_b^{0(-)} \rightarrow \Xi_c(3055)^{+(0)}\pi^-$ decays, and the relative branching fractions for $\Xi_c(3080)^{+(0)}$ and $\Xi_c(3055)^{+(0)}$ baryons (R_B). All results are obtained under the favored hypothesis $J_{\Xi_c(3055)^{+(0)}}^P = 3/2^+$. The first uncertainties are statistical and the second are systematic.

Quantity	$\Xi_c(3055)^+$	$\Xi_c(3055)^0$
m [MeV/ c^2]	$3054.52 \pm 0.36 \pm 0.17$	$3061.00 \pm 0.80 \pm 0.23$
Γ [MeV/ c^2]	$8.01 \pm 0.76 \pm 0.34$	$12.4 \pm 2.0 \pm 1.1$
α	$-0.92 \pm 0.10 \pm 0.05$	$-0.92 \pm 0.16 \pm 0.22$
R_B	$0.045 \pm 0.023 \pm 0.006$	$0.14 \pm 0.06 \pm 0.04$

hold, the up-down asymmetry is close to -1 [55–57]. The $\Xi_b^0 \rightarrow \Xi_c(3055)^+\pi^-$ decay is such a process in the case that $\Xi_c(3055)^+$ baryon is the D -wave λ -excitation. Otherwise, if the $\Xi_c(3055)^+$ baryon is a $6F$ state, the up-down asymmetry could depart strongly from -1 [58]. The up-down asymmetries measured under other $J_{\Xi_c(3055)^+}^P$ hypotheses are listed in Table 2, where $J_{\Xi_c(3080)^+}^P = 5/2^+$ and $J_{\text{NR}}^P = 1/2^-$ are fixed. Under the favored hypothesis $J_{\Xi_c(3055)^+}^P = 3/2^+$, $\alpha = -0.92 \pm 0.10 \pm 0.05$ is consistent with maximal parity violation, which is not the case for other J^P assignments.

The same analysis is carried out for the $\Xi_b^- \rightarrow \Xi_c(3055)^0\pi^-$ channel, where $J_{\Xi_c(3055)^0}^P = 3/2^+$ is also favored, and yields $\alpha = -0.92 \pm 0.16 \pm 0.22$ under this hypothesis. The corresponding fit projections on data distributions are shown in Fig. 3. The measured properties for both channels are summarized in Table 1.

The significances of favoring $J_{\Xi_c(3055)^{+(0)}}^P = 3/2^+$ over another hypothesis are evaluated with a likelihood-ratio test on pseudoexperiments. Samples are generated with an alternative J_{alt}^P for the $\Xi_c(3055)^{+(0)}$ baryons and fits are performed with $J^P = 3/2^+$ and J_{alt}^P hypotheses. The difference between twice the log \mathcal{L} values of the two fits is taken as the test statistic t . The t distribution of pseudoexperiments is approximated by a Gaussian function with $\mu(t_{J_{\text{alt}}^P})$ and $\sigma(t_{J_{\text{alt}}^P})$ as the mean and standard deviation, respectively. The $J^P = 3/2^+$ hypothesis is favored over the J_{alt}^P hypothesis by a significance calculated as

$$n_\sigma(J_{\text{alt}}^P) = \frac{t_{\text{data}} - \mu(t_{J_{\text{alt}}^P})}{\sigma(t_{J_{\text{alt}}^P})}, \quad (5)$$

where t_{data} is the test statistic for data. Among all tested hypotheses, the minimum significance of the $J_{\Xi_c(3055)^{+(0)}}^P = 3/2^+$ hypothesis is 6.5σ (3.5σ) against the $J_{\text{alt}}^P = 5/2^-$ ($3/2^-$) hypothesis. The t distributions of pseudoexperiments generated with $J_{\Xi_c(3055)^{+(0)}}^P = 3/2^+$ and $5/2^-$ ($3/2^-$) are shown in Fig. 4, compared with the test statistic in data. The significances of the $J_{\Xi_c(3055)^{+(0)}}^P = 3/2^+$ hypothesis over all the tested alternative hypotheses are listed in Table 2. Given the $\Xi_c(3055)^+$ and $\Xi_c(3055)^0$ baryons are assumed to be isospin partners, the $J_{\Xi_c(3055)^{+(0)}}^P = 3/2^+$ hypothesis is well established by these measurements.

Systematic uncertainties on the masses and widths of the $\Xi_c(3055)^{+(0)}$ baryons, the up-down asymmetries of the $\Xi_b^{0(-)} \rightarrow \Xi_c(3055)^{+(0)}\pi^-$ transitions as well as the relative branching fractions R_B are listed in Tables 3 and 4 in Appendix 2. Possible biases introduced by the amplitude fit are evaluated using pseudoexperiments, and are corrected

Table 2: Tested spin-parity hypotheses and the significance of favoring $J_{\Xi_c(3055)^+(0)}^P = 3/2^+$ over each hypothesis, n_σ . Measured up-down asymmetries α in the $\Xi_b^{0(-)} \rightarrow \Xi_c(3055)^+(0)\pi^-$ decays are also given, with statistical uncertainties.

$J_{\Xi_c(3055)^+(0)}^P$	n_σ	α
$1/2^-$	12.9 (6.5)	-0.10 ± 0.17 (-0.63 ± 0.28)
$1/2^+$	11.0 (5.5)	$+0.31 \pm 0.13$ ($+0.32 \pm 0.20$)
$3/2^-$	7.3 (3.5)	$+0.18 \pm 0.14$ ($+0.20 \pm 0.23$)
$5/2^-$	6.5 (4.8)	-0.12 ± 0.14 (-0.21 ± 0.23)
$5/2^+$	9.8 (4.8)	$+0.52 \pm 0.14$ ($+0.30 \pm 0.27$)
$7/2^-$	10.7 (6.2)	$+0.41 \pm 0.16$ ($+0.19 \pm 0.22$)
$7/2^+$	10.9 (6.0)	$+0.12 \pm 0.14$ (-0.30 ± 0.25)

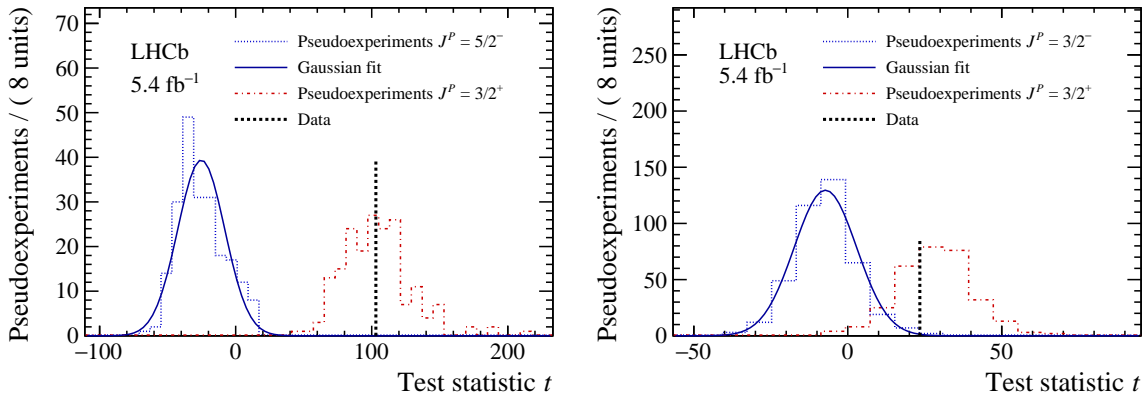


Figure 4: Distributions of the test statistic for (blue) pseudoexperiments generated with the alternative hypotheses of (left) $J_{\text{alt}}^P = 5/2^-$ for the $\Xi_c(3055)^+$ baryon and (right) $J_{\text{alt}}^P = 3/2^-$ for the $\Xi_c(3055)^0$ baryon. Distributions for (red) pseudoexperiments generated with the $J^P = 3/2^+$ hypothesis are also plotted as comparison. Values of the test statistic in data are also given.

for in the measurements. The uncertainties on the known masses of the Λ , $D^{+(0)}$ and π^- hadrons [44] are propagated to the $\Xi_c(3055)^+(0)$ mass measurement. Momentum-scale calibration for charged particles yields an uncertainty on the $\Xi_c(3055)^+(0)$ mass measurements [59]. The experimental resolution smears the $m_{D^{+(0)}\Lambda}$ invariant-mass distribution, and introduces an uncertainty on the masses. The limited size of the simulation sample used for the PDF normalization results in an uncertainty, which is evaluated using the bootstrap method [60]. Corrections are applied to simulation to match the trigger performances in data, and the uncertainty on this correction leads to a systematic uncertainty. The $\Xi_b^{0(-)}$ candidates are reconstructed in two categories, depending on whether the Λ baryon decays within or downstream of the LHCb vertex detector [61]. The possible efficiency difference between them is studied as a source of systematic uncertainty. In the fit to the invariant-mass distribution of the $\Xi_b^{0(-)}$ baryon, the models for the signal, the combinatorial and the partially reconstructed background are varied to evaluate the corresponding systematic uncertainty. The orbital angular momentum between the $\Xi_c^{+(0)}$ baryon and the π^- meson in the $\Xi_b^{0(-)} \rightarrow \Xi_c^{+(0)}\pi^-$ decay is

fixed to the lowest value in the baseline amplitude fit, and a systematic uncertainty is evaluated by considering all possible values. An exponential function is used to describe the nonresonant invariant-mass distribution. An alternative linear function is tested, and the difference from the baseline result is taken as an uncertainty. The fixed $\Xi_c(3080)^{+(0)}$ masses and widths are varied within their uncertainties, resulting in two sources of systematic uncertainties. It is possible that the same track segment is shared by more than one track in the $\Xi_b^{0(-)}$ final state, resulting in cloned tracks. The results obtained by removing such candidates are compared with the baseline results and the differences are quoted as systematic uncertainties. In total, the systematic uncertainties are comparable to the statistical uncertainties.

In conclusion, the $\Xi_b^{0(-)} \rightarrow \Xi_c(3055)^{+(0)}\pi^-$ decays, with $\Xi_c(3055)^{+(0)} \rightarrow D^{+(0)}\Lambda$ are observed for the first time in pp collisions using data recorded at $\sqrt{s} = 13$ TeV, corresponding to an integrated luminosity of 5.4 fb^{-1} . An amplitude analysis is performed on each channel independently, determining for the first time the spin-parity of the $\Xi_c(3055)^{+(0)}$ baryons to be $3/2^+$, with significances of more than 6.5σ (3.5σ) against other hypotheses. Different sources of systematic uncertainties have been taken into account, and the minimum significance among the alternative results is chosen. With the spin-parity assignment of $J^P = 3/2^+$, the up-down asymmetries of the $\Xi_b^{0(-)} \rightarrow \Xi_c(3055)^{+(0)}\pi^-$ decays are measured to be -0.92 ± 0.10 (stat) ± 0.05 (syst) (-0.92 ± 0.16 (stat) ± 0.22 (syst)), consistent with maximal parity violation. This is the first measurement of the parity-violating parameter for the transition of the $\Xi_b^{0(-)}$ baryon to a $\Xi_c^{+(0)}$ baryon and a pseudoscalar meson. The result supports the factorization approximation in color-allowed beauty-to-charm baryon decays, which indicates the structure of the $\Xi_c(3055)^{+(0)}$ state. The masses and widths of the $\Xi_c(3055)^{+(0)}$ baryons are also measured, with a precision comparable to known results [44]. All the obtained results for the $\Xi_c(3055)^{+(0)}$ state support its interpretation as the first D -wave excitation of the flavor antisymmetric $\bar{3}_F \Xi_c$ state. The significances of the $\Xi_b^{0(-)} \rightarrow \Xi_c(3080)^{+(0)}(\rightarrow D^{+(0)}\Lambda)\pi^-$ signal are determined to be 4.4σ (3.6σ), and their branching fractions relative to those of the $\Xi_b^{0(-)} \rightarrow \Xi_c(3055)^{+(0)}(\rightarrow D^{+(0)}\Lambda)\pi^-$ decays are measured for the first time.

Acknowledgements

We express our gratitude to our colleagues in the CERN accelerator departments for the excellent performance of the LHC. We thank the technical and administrative staff at the LHCb institutes. We acknowledge support from CERN and from the national agencies: CAPES, CNPq, FAPERJ and FINEP (Brazil); MOST and NSFC (China); CNRS/IN2P3 (France); BMBF, DFG and MPG (Germany); INFN (Italy); NWO (Netherlands); MNiSW and NCN (Poland); MCID/IFA (Romania); MICIU and AEI (Spain); SNSF and SER (Switzerland); NASU (Ukraine); STFC (United Kingdom); DOE NP and NSF (USA). We acknowledge the computing resources that are provided by CERN, IN2P3 (France), KIT and DESY (Germany), INFN (Italy), SURF (Netherlands), PIC (Spain), GridPP (United Kingdom), CSCS (Switzerland), IFIN-HH (Romania), CBPF (Brazil), and Polish WLCG (Poland). We are indebted to the communities behind the multiple open-source software packages on which we depend. Individual groups or members have received support from ARC and ARDC (Australia); Key Research Program of Frontier Sciences of CAS, CAS PIFI, CAS CCEPP, Fundamental Research Funds for the Central Universities, and Sci.

& Tech. Program of Guangzhou (China); Minciencias (Colombia); EPLANET, Marie Skłodowska-Curie Actions, ERC and NextGenerationEU (European Union); A*MIDEX, ANR, IPhU and Labex P2IO, and Région Auvergne-Rhône-Alpes (France); AvH Foundation (Germany); ICSC (Italy); Severo Ochoa and María de Maeztu Units of Excellence, GVA, XuntaGal, GENCAT, InTalent-Inditex and Prog. Atracción Talento CM (Spain); SRC (Sweden); the Leverhulme Trust, the Royal Society and UKRI (United Kingdom).

End matter

1 Formula of the amplitude model

The full formula of the amplitude model used to describe $\Xi_b \rightarrow \Xi_c \pi^-$ decays is

$$\mathcal{M}_{\lambda_{\Xi_b}, \lambda_p}(m_{D\Lambda}, \vec{\Omega}|\vec{v}) = \sum_{\Xi_c} \sum_{\lambda_A = \pm \frac{1}{2}} (-1)^{J+1/2} \times P \times H_{\lambda_{\Xi_b}}^{\Xi_b} \times H_{\lambda_p}^{\Lambda} \times d_{\lambda_{\Xi_b}, \lambda_A}^J(\theta_{\Xi_c}) d_{\lambda_A, \lambda_p}^{1/2}(\beta_A) e^{i\phi_A \lambda_A} R(m_{D\Lambda}),$$

where the Ξ_c refers to the $\Xi_c(3055)$ and $\Xi_c(3080)$ resonances, as well as the nonresonant component for simplicity, λ is the helicity of a given particle, and H is the helicity coupling of the corresponding decay. The $\Xi_c \rightarrow D\Lambda$ strong decay contributes to a $(-1)^{J+1/2}$ term, assuming parity is conserved in such decays. Finally, J and P are the spin and parity of the Ξ_c baryon, d is the Wigner small- d function, and the $R(m_{D\Lambda})$ terms are Breit–Wigner functions convoluted with a Gaussian function for the Ξ_c signal, and exponential functions for nonresonant background.

The definition of the decay angles is illustrated in Fig. 5.

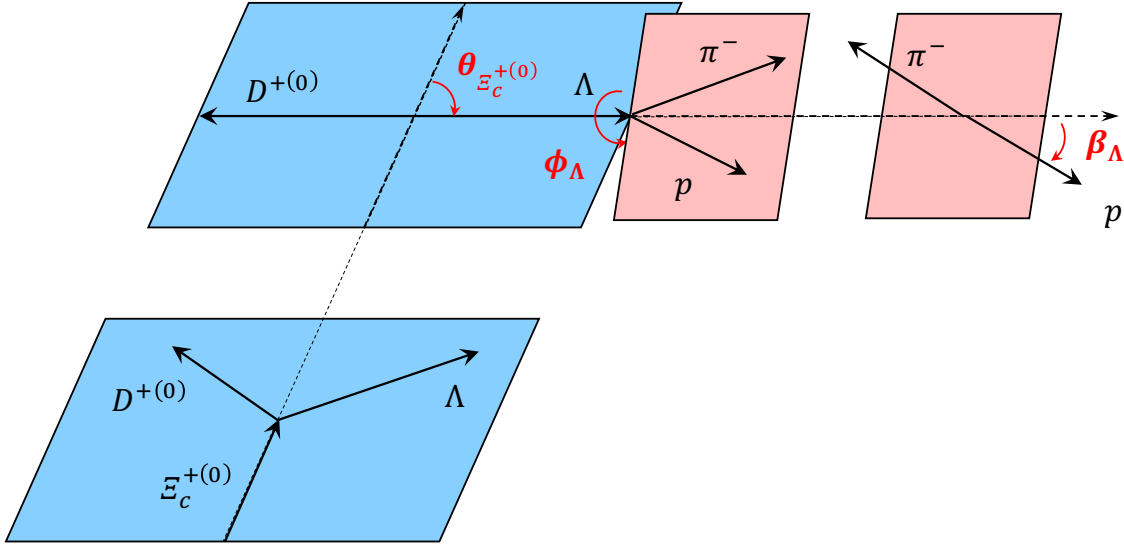


Figure 5: Definition of the three angular variables $\cos \theta_{\Xi_c}$, ϕ_Λ and $\cos \beta_\Lambda$. The variable θ_{Ξ_c} is the angle between the Λ momentum in the rest frame of the $D\Lambda$ system (denoted as Ξ_c) and the Ξ_c momentum in the Ξ_b^0 rest frame, referred as the Ξ_c helicity angle. The Λ helicity angle β_Λ is the angle between the p momentum in the Λ rest frame and the Λ momentum in the Ξ_c rest frame. The variable ϕ_Λ is the angle between the $\Xi_c \rightarrow D\Lambda$ and $\Lambda \rightarrow p\pi^-$ decay planes.

2 Summary table of systematic uncertainties

The biases and systematic uncertainties on the masses (m) and widths (Γ) for the $\Xi_c(3055)^{+(0)}$ baryons, the up-down asymmetries (α) of the $\Xi_b^{0(-)} \rightarrow \Xi_c(3055)^{+(0)}\pi^-$ decays, and the relative branching fractions for $\Xi_c(3080)^{+(0)}$ and $\Xi_c(3055)^{+(0)}$ baryons (R_B) are summarized in Tables 3 and 4.

Table 3: Biases and systematic uncertainties for the $\Xi_b^0 \rightarrow \Xi_c(3055)^+\pi^-$ channel.

Source	σ_m [MeV/ c^2]	σ_Γ [MeV/ c^2]	σ_α	σ_{R_B}
Amplitude fit bias	–	–	–	–
Hadron masses	± 0.05	–	–	–
Momentum scale	± 0.01	–	–	–
Resolution	± 0.00	± 0.07	± 0.00	± 0.000
Simulation sample	± 0.15	± 0.30	± 0.02	± 0.002
Trigger correction	± 0.01	± 0.03	± 0.02	± 0.000
Λ categories	± 0.03	± 0.04	± 0.01	± 0.002
Ξ_b^0 mass fit model	± 0.03	± 0.13	± 0.01	± 0.001
Angular momentum	± 0.00	± 0.00	± 0.04	± 0.002
Nonresonant model	± 0.00	± 0.00	± 0.00	± 0.000
$\Xi_c(3080)^+$ width	± 0.01	± 0.01	± 0.00	± 0.003
$\Xi_c(3080)^+$ mass	± 0.00	± 0.02	± 0.00	± 0.000
Clone tracks	± 0.02	± 0.03	± 0.01	± 0.003
Total	± 0.17	± 0.34	± 0.05	± 0.006

Table 4: Biases and systematic uncertainties for the $\Xi_b^- \rightarrow \Xi_c(3055)^0\pi^-$ channel.

Source	σ_m [MeV/ c^2]	σ_Γ [MeV/ c^2]	σ_α	σ_{R_B}
Amplitude fit bias	–	–0.46	–	–
Hadron masses	± 0.05	–	–	–
Momentum scale	± 0.03	–	–	–
Resolution	± 0.00	± 0.10	± 0.00	± 0.001
Simulation sample	± 0.13	± 0.38	± 0.02	± 0.006
Trigger correction	± 0.01	± 0.03	± 0.00	± 0.001
Λ categories	± 0.04	± 0.12	± 0.05	± 0.004
Ξ_b^- mass fit model	± 0.00	± 0.19	± 0.02	± 0.003
Angular momentum	± 0.01	± 0.15	± 0.21	± 0.014
Nonresonant model	± 0.00	± 0.03	± 0.00	± 0.001
$\Xi_c(3080)^0$ width	± 0.08	± 0.69	± 0.01	± 0.032
$\Xi_c(3080)^0$ mass	± 0.03	± 0.20	± 0.01	± 0.006
Clone tracks	± 0.13	± 0.04	± 0.04	± 0.008
Total	± 0.23	± 1.11	± 0.22	± 0.038

References

- [1] N. Isgur and M. B. Wise, *Spectroscopy with heavy quark symmetry*, *Phys. Rev. Lett.* **66** (1991) 1130.
- [2] H.-X. Chen *et al.*, *An updated review of the new hadron states*, *Rept. Prog. Phys.* **86** (2023) 026201, [arXiv:2204.02649](#).
- [3] H.-X. Chen *et al.*, *A review of the open charm and open bottom systems*, *Rept. Prog. Phys.* **80** (2017) 076201, [arXiv:1609.08928](#).
- [4] Belle collaboration, R. Mizuk *et al.*, *Observation of an isotriplet of excited charmed baryons decaying to $\Lambda_c^+\pi$* , *Phys. Rev. Lett.* **94** (2005) 122002, [arXiv:hep-ex/0412069](#).
- [5] Belle collaboration, R. Chistov *et al.*, *Observation of new states decaying into $\Lambda_c^+K^-\pi^+$ and $\Lambda_c^+K_S^0\pi^-$* , *Phys. Rev. Lett.* **97** (2006) 162001, [arXiv:hep-ex/0606051](#).
- [6] Belle collaboration, K. Abe *et al.*, *Experimental constraints on the spin and parity of the $\Lambda_c(2880)^+$* , *Phys. Rev. Lett.* **98** (2007) 262001, [arXiv:hep-ex/0608043](#).
- [7] Belle collaboration, T. Lesiak *et al.*, *Measurement of masses of the $\Xi_c(2645)$ and $\Xi_c(2815)$ baryons and observation of $\Xi_c(2980) \rightarrow \Xi_c(2645)\pi$* , *Phys. Lett.* **B665** (2008) 9, [arXiv:0802.3968](#).
- [8] E. Solovieva *et al.*, *Study of Ω_c^0 and Ω_c^{*0} baryons at Belle*, *Phys. Lett.* **B672** (2009) 1, [arXiv:0808.3677](#).
- [9] Belle collaboration, Y. Kato *et al.*, *Search for doubly charmed baryons and study of charmed strange baryons at Belle*, *Phys. Rev.* **D89** (2014) 052003, [arXiv:1312.1026](#).
- [10] Belle collaboration, Y. Kato *et al.*, *Studies of charmed strange baryons in the ΛD final state at Belle*, *Phys. Rev.* **D94** (2016) 032002, [arXiv:1605.09103](#).
- [11] Belle collaboration, J. Yelton *et al.*, *Observation of excited Ω_c charmed baryons in e^+e^- collisions*, *Phys. Rev.* **D97** (2018) 051102, [arXiv:1711.07927](#).
- [12] BaBar collaboration, B. Aubert *et al.*, *Observation of an excited charm baryon Ω_c^* decaying to $\Omega_c^0\gamma$* , *Phys. Rev. Lett.* **97** (2006) 232001, [arXiv:hep-ex/0608055](#).
- [13] BaBar collaboration, B. Aubert *et al.*, *Observation of a charmed baryon decaying to D^0p at a mass near $2.94 \text{ GeV}/c^2$* , *Phys. Rev. Lett.* **98** (2007) 012001, [arXiv:hep-ex/0603052](#).
- [14] BaBar collaboration, B. Aubert *et al.*, *A study of excited charm-strange baryons with evidence for new baryons $\Xi_c(3055)^+$ and $\Xi_c(3123)^+$* , *Phys. Rev.* **D77** (2008) 012002, [arXiv:0710.5763](#).
- [15] LHCb collaboration, R. Aaij *et al.*, *Observation of five new narrow Ω_c^0 states decaying to $\Xi_c^+K^-$* , *Phys. Rev. Lett.* **118** (2017) 182001, [arXiv:1703.04639](#).
- [16] LHCb collaboration, R. Aaij *et al.*, *Observation of excited Ω_c^0 baryons in $\Omega_b^- \rightarrow \Xi_c^+K^-\pi^+$ decays*, *Phys. Rev.* **D104** (2021) L091102, [arXiv:2107.03419](#).






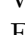
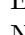
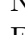
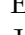

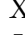






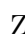
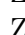
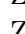
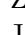
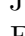
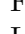
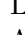
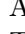
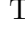
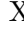
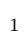
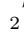
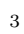

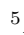
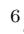


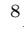
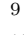
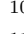
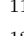
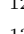
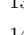

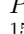
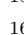
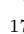
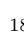
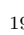
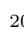
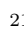
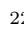
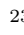
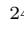
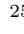
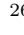







- [17] LHCb collaboration, R. Aaij *et al.*, *Observation of new Ω_c^0 states decaying to the $\Xi_c^+ K^-$ final state*, *Phys. Rev. Lett.* **131** (2023) 131902, [arXiv:2302.04733](#).
- [18] X. Liu, C. Chen, W.-Z. Deng, and X.-L. Chen, *A note on $\Xi_c(3055)^+$ and $\Xi_c(3123)^+$* , *Chin. Phys.* **C32** (2008) 424, [arXiv:0710.0187](#).
- [19] X.-H. Guo, K.-W. Wei, and X.-H. Wu, *Some mass relations for mesons and baryons in Regge phenomenology*, *Phys. Rev.* **D78** (2008) 056005, [arXiv:0809.1702](#).
- [20] L.-H. Liu, L.-Y. Xiao, and X.-H. Zhong, *Charm-strange baryon strong decays in a chiral quark model*, *Phys. Rev.* **D86** (2012) 034024, [arXiv:1205.2943](#).
- [21] B. Chen, K.-W. Wei, and A. Zhang, *Assignments of Λ_Q and Ξ_Q baryons in the heavy quark-light diquark picture*, *Eur. Phys. J.* **A51** (2015) 82, [arXiv:1406.6561](#).
- [22] H.-X. Chen *et al.*, *D-wave charmed and bottomed baryons from QCD sum rules*, *Phys. Rev.* **D94** (2016) 114016.
- [23] Z. Zhao, D.-D. Ye, and A. Zhang, *Nature of charmed strange baryons $\Xi_c(3055)$ and $\Xi_c(3080)$* , *Phys. Rev.* **D94** (2016) 114020, [arXiv:1608.04856](#).
- [24] B. Chen, X. Liu, and A. Zhang, *Newly observed $\Lambda_c(2860)^+$ at LHCb and its D-wave partners $\Lambda_c(2880)^+$, $\Xi_c(3055)^+$ and $\Xi_c(3080)^+$* , *Phys. Rev.* **D95** (2017) 074022, [arXiv:1702.04106](#).
- [25] Z.-G. Wang, *The $\Lambda_c(2860)$, $\Lambda_c(2880)$, $\Xi_c(3055)$ and $\Xi_c(3080)$ as D-wave baryon states in QCD*, *Nucl. Phys.* **B926** (2018) 467, [arXiv:1705.07745](#).
- [26] D.-D. Ye, Z. Zhao, and A. Zhang, *Study of 2S- and 1D- excitations of observed charmed strange baryons*, *Phys. Rev.* **D96** (2017) 114003, [arXiv:1710.10165](#).
- [27] Y.-X. Yao, K.-L. Wang, and X.-H. Zhong, *Strong and radiative decays of the low-lying D-wave singly heavy baryons*, *Phys. Rev.* **D98** (2018) 076015, [arXiv:1803.00364](#).
- [28] Q.-X. Yu, R. Pavao, V. R. Debastiani, and E. Oset, *Description of the Ξ_c and Ξ_b states as molecular states*, *Eur. Phys. J.* **C79** (2019) 167, [arXiv:1811.11738](#).
- [29] M. Jacob and G. C. Wick, *On the general theory of collisions for particles with spin*, *Annals Phys.* **7** (1959) 404.
- [30] LHCb collaboration, A. A. Alves Jr. *et al.*, *The LHCb detector at the LHC*, *JINST* **3** (2008) S08005.
- [31] LHCb collaboration, R. Aaij *et al.*, *LHCb detector performance*, *Int. J. Mod. Phys.* **A30** (2015) 1530022, [arXiv:1412.6352](#).
- [32] R. Aaij *et al.*, *The LHCb trigger and its performance in 2011*, *JINST* **8** (2013) P04022, [arXiv:1211.3055](#).
- [33] LHCb collaboration, *LHCb Trigger and Online Upgrade Technical Design Report*, [CERN-LHCC-2014-016](#), 2014.

- [34] T. Likhomanenko *et al.*, *LHCb topological trigger reoptimization*, *J. Phys. Conf. Ser.* **664** (2015) 082025, [arXiv:1510.00572](#).
- [35] V. V. Gligorov and M. Williams, *Efficient, reliable and fast high-level triggering using a bonsai boosted decision tree*, *JINST* **8** (2013) P02013, [arXiv:1210.6861](#).
- [36] R. Aaij *et al.*, *Design and performance of the LHCb trigger and full real-time reconstruction in Run 2 of the LHC*, *JINST* **14** (2019) P04013, [arXiv:1812.10790](#).
- [37] T. Sjöstrand, S. Mrenna, and P. Skands, *A brief introduction to PYTHIA 8.1*, *Comput. Phys. Commun.* **178** (2008) 852, [arXiv:0710.3820](#); T. Sjöstrand, S. Mrenna, and P. Skands, *PYTHIA 6.4 physics and manual*, *JHEP* **05** (2006) 026, [arXiv:hep-ph/0603175](#).
- [38] I. Belyaev *et al.*, *Handling of the generation of primary events in Gauss, the LHCb simulation framework*, *J. Phys. Conf. Ser.* **331** (2011) 032047.
- [39] D. J. Lange, *The EvtGen particle decay simulation package*, *Nucl. Instrum. Meth.* **A462** (2001) 152.
- [40] N. Davidson, T. Przedzinski, and Z. Was, *PHOTOS interface in C++: Technical and physics documentation*, *Comp. Phys. Comm.* **199** (2016) 86, [arXiv:1011.0937](#).
- [41] Geant4 collaboration, J. Allison *et al.*, *Geant4 developments and applications*, *IEEE Trans. Nucl. Sci.* **53** (2006) 270; Geant4 collaboration, S. Agostinelli *et al.*, *Geant4: A simulation toolkit*, *Nucl. Instrum. Meth.* **A506** (2003) 250.
- [42] M. Clemencic *et al.*, *The LHCb simulation application, Gauss: Design, evolution and experience*, *J. Phys. Conf. Ser.* **331** (2011) 032023.
- [43] G. A. Cowan, D. C. Craik, and M. D. Needham, *RapidSim: an application for the fast simulation of heavy-quark hadron decays*, *Comput. Phys. Commun.* **214** (2017) 239, [arXiv:1612.07489](#).
- [44] Particle Data Group, N. S. *et al.*, *Review of particle physics*, to be published in *Phys. Rev* **D110** (2024) 030001.
- [45] W. D. Hulsbergen, *Decay chain fitting with a Kalman filter*, *Nucl. Instrum. Meth.* **A552** (2005) 566, [arXiv:physics/0503191](#).
- [46] A. Hoecker *et al.*, *TMVA 4 — Toolkit for Multivariate Data Analysis with ROOT. Users Guide.*, [arXiv:physics/0703039](#).
- [47] T. Skwarnicki, *A study of the radiative cascade transitions between the Upsilon-prime and Upsilon resonances*, PhD thesis, Institute of Nuclear Physics, Krakow, 1986, [DESY-F31-86-02](#).
- [48] M. Pivk and F. R. Le Diberder, *sPlot: A statistical tool to unfold data distributions*, *Nucl. Instrum. Meth.* **A555** (2005) 356, [arXiv:physics/0402083](#).
- [49] LHCb collaboration, R. Aaij *et al.*, *Measurement of the $\Lambda_b^0 \rightarrow J/\psi\Lambda$ angular distribution and the Λ polarisation in pp collisions*, *JHEP* **06** (2020) 110, [arXiv:2004.10563](#).

- [50] Y. Xie, *sFit: a method for background subtraction in maximum likelihood fit*, [arXiv:0905.0724](#).
- [51] C. Langenbruch, *Parameter uncertainties in weighted unbinned maximum likelihood fits*, *Eur. Phys. J.* **C82** (2022) 393, [arXiv:1911.01303](#).
- [52] R. E. Caflisch, *Monte Carlo and quasi-Monte Carlo methods*, *Acta Numerica* **7** (1998) 1.
- [53] T.-D. Lee and C.-N. Yang, *Question of parity conservation in weak interactions*, *Phys. Rev.* **104** (1956) 254.
- [54] BESIII collaboration, M. Ablikim *et al.*, *Precise measurements of decay parameters and CP asymmetry with entangled $\Lambda - \bar{\Lambda}$ pairs*, *Phys. Rev. Lett.* **129** (2022) 131801, [arXiv:2204.11058](#).
- [55] H.-Y. Cheng, *Nonleptonic weak decays of bottom baryons*, *Phys. Rev.* **D56** (1997) 2799, [arXiv:hep-ph/9612223](#), [Erratum: *Phys.Rev.D* 99, 079901 (2019)].
- [56] C.-K. Chua, *Color-allowed bottom baryon to charmed baryon nonleptonic decays*, *Phys. Rev.* **D99** (2019) 014023, [arXiv:1811.09265](#).
- [57] Y.-S. Li and X. Liu, *Investigating the transition form factors of $\Lambda_b^0 \rightarrow \Lambda_c(2625)$ and $\Xi_b \rightarrow \Xi_c(2815)$ and the corresponding weak decays with support from baryon spectroscopy*, *Phys. Rev.* **D107** (2023) 033005, [arXiv:2212.00300](#).
- [58] H.-W. Ke, G.-Y. Fang, and Y.-L. Shi, *Study on the mixing of Ξ_c and Ξ_c' by the transition $\Xi_b \rightarrow \Xi_c^{(\prime)}$* , *Phys. Rev.* **D109** (2024) 073006, [arXiv:2401.11106](#).
- [59] LHCb collaboration, R. Aaij *et al.*, *Momentum scale calibration of the LHCb spectrometer*, *JINST* **19** (2024) P02008, [arXiv:2312.01772](#).
- [60] B. Efron, *Bootstrap methods: Another look at the jackknife*, *Ann. Statist.* **7** (1979) 1.
- [61] R. Aaij *et al.*, *Performance of the LHCb Vertex Locator*, *JINST* **9** (2014) P09007, [arXiv:1405.7808](#).

LHCb collaboration

R. Aaij³⁶, A.S.W. Abdelmotteleb⁵⁵, C. Abellan Beteta⁴⁹, F. Abudinén⁵⁵,
T. Ackernley⁵⁹, A. A. Adefisoye⁶⁷, B. Adeva⁴⁵, M. Adinolfi⁵³, P. Adlarson⁸⁰,
C. Agapopoulou¹³, C.A. Aidala⁸¹, Z. Ajaltouni¹¹, S. Akar⁶⁴, K. Akiba³⁶,
P. Albicocco²⁶, J. Albrecht¹⁸, F. Alessio⁴⁷, M. Alexander⁵⁸, Z. Aliouche⁶¹,
P. Alvarez Cartelle⁵⁴, R. Amalric¹⁵, S. Amato³, J.L. Amey⁵³, Y. Amhis^{13,47},
L. An⁶, L. Anderlini²⁵, M. Andersson⁴⁹, A. Andreianov⁴², P. Andreola⁴⁹,
M. Andreotti²⁴, D. Andreou⁶⁷, A. Anelli^{29,n}, D. Ao⁷, F. Archilli^{35,t},
M. Argenton²⁴, S. Arguedas Cuendis^{9,47}, A. Artamonov⁴², M. Artuso⁶⁷,
E. Aslanides¹², R. Ataíde Da Silva⁴⁸, M. Atzeni⁶³, B. Audurier¹⁴, D. Bacher⁶²,
I. Bachiller Perea¹⁰, S. Bachmann²⁰, M. Bachmayer⁴⁸, J.J. Back⁵⁵,
P. Baladron Rodriguez⁴⁵, V. Balagura¹⁴, W. Baldini²⁴, L. Balzani¹⁸, H. Bao⁷,
J. Baptista de Souza Leite⁵⁹, C. Barbero Pretel^{45,82}, M. Barbetti²⁵, I. R. Barbosa⁶⁸,
R.J. Barlow⁶¹, M. Barnyakov²³, S. Barsuk¹³, W. Barter⁵⁷, M. Bartolini⁵⁴,
J. Bartz⁶⁷, J.M. Basels¹⁶, S. Bashir³⁸, G. Bassi^{33,q}, B. Batsukh⁵, P. B. Battista¹³,
A. Bay⁴⁸, A. Beck⁵⁵, M. Becker¹⁸, F. Bedeschi³³, I.B. Bediaga², N. A. Behling¹⁸,
S. Belin⁴⁵, V. Bellec⁴⁹, K. Belous⁴², I. Belov²⁷, I. Belyaev³⁴, G. Benane¹²,
G. Bencivenni²⁶, E. Ben-Haim¹⁵, A. Berezhnoy⁴², R. Bernet⁴⁹, S. Bernet Andres⁴³,
A. Bertolin³¹, C. Betancourt⁴⁹, F. Betti⁵⁷, J. Bex⁵⁴, Ia. Bezshyiko⁴⁹, J. Bhom³⁹,
M.S. Bieker¹⁸, N.V. Biesuz²⁴, P. Billoir¹⁵, A. Biolchini³⁶, M. Birch⁶⁰,
F.C.R. Bishop¹⁰, A. Bitadze⁶¹, A. Bizzeti⁴⁹, T. Blake⁵⁵, F. Blanc⁴⁸, J.E. Blank¹⁸,
S. Blusk⁶⁷, V. Bocharnikov⁴², J.A. Boelhaue¹⁸, O. Boente Garcia¹⁴,
T. Boettcher⁶⁴, A. Bohare⁵⁷, A. Boldyrev⁴², C.S. Bolognani⁷⁷, R. Bolzonella^{24,k},
N. Bondar⁴², A. Bordelius⁴⁷, F. Borgato^{31,o}, S. Borghi⁶¹, M. Borsato^{29,n},
J.T. Borsuk³⁹, S.A. Bouchiba⁴⁸, M. Bovill⁶², T.J.V. Bowcock⁵⁹, A. Boyer⁴⁷,
C. Bozzi²⁴, A. Brea Rodriguez⁴⁸, N. Breer¹⁸, J. Brodzicka³⁹,
A. Brossa Gonzalo^{45,55,44,†}, J. Brown⁵⁹, D. Brundu³⁰, E. Buchanan⁵⁷, A. Buonauro⁴⁹,
L. Buonincontri^{31,o}, A.T. Burke⁶¹, C. Burr⁴⁷, A. Butkevich⁴², J.S. Butter⁵⁴,
J. Buytaert⁴⁷, W. Byczynski⁴⁷, S. Cadeddu³⁰, H. Cai⁷², A. C. Caillet¹⁵,
R. Calabrese^{24,k}, S. Calderon Ramirez⁹, L. Calefice⁴⁴, S. Cali²⁶, M. Calvi^{29,n},
M. Calvo Gomez⁴³, P. Camargo Magalhaes^{2,x}, J. I. Cambon Bouzas⁴⁵, P. Campana²⁶,
D.H. Campora Perez⁷⁷, A.F. Campoverde Quezada⁷, S. Capelli²⁹, L. Capriotti²⁴,
R. Caravaca-Mora⁹, A. Carbone^{23,i}, L. Carcedo Salgado⁴⁵, R. Cardinale^{27,l},
A. Cardini³⁰, P. Carniti^{29,n}, L. Carus²⁰, A. Casais Vidal⁶³, R. Caspary²⁰,
G. Casse⁵⁹, J. Castro Godinez⁹, M. Cattaneo⁴⁷, G. Cavallero^{24,47}, V. Cavallini^{24,k},
S. Celani²⁰, D. Cervenkov⁶², S. Cesare^{28,m}, A.J. Chadwick⁵⁹, I. Chahrour⁸¹,
M. Charles¹⁵, Ph. Charpentier⁴⁷, E. Chatzianagnostou³⁶, C.A. Chavez Barajas⁵⁹,
M. Chefdeville¹⁰, C. Chen¹², S. Chen⁵, Z. Chen⁷, A. Chernov³⁹,
S. Chernyshenko⁵¹, X. Chiotopoulos⁷⁷, V. Chobanova⁷⁹, S. Cholak⁴⁸,
M. Chrzaszcz³⁹, A. Chubykin⁴², V. Chulikov⁴², P. Ciambrone²⁶, X. Cid Vidal⁴⁵,
G. Ciezarek⁴⁷, P. Cifra⁴⁷, P.E.L. Clarke⁵⁷, M. Clemencic⁴⁷, H.V. Cliff⁵⁴,
J. Closier⁴⁷, C. Cocha Toapaxi²⁰, V. Coco⁴⁷, J. Cogan¹², E. Cogneras¹¹,
L. Cojocariu⁴¹, P. Collins⁴⁷, T. Colombo⁴⁷, M. C. Colonna¹⁸,
A. Comerma-Montells⁴⁴, L. Congedo²², A. Contu³⁰, N. Cooke⁵⁸, I. Corredoira⁴⁵,
A. Correia¹⁵, G. Corti⁴⁷, J.J. Cottee Meldrum⁵³, B. Couturier⁴⁷, D.C. Craik⁴⁹,
M. Cruz Torres^{2,f}, E. Curras Rivera⁴⁸, R. Currie⁵⁷, C.L. Da Silva⁶⁶, S. Dadabaev⁴²,
L. Dai⁶⁹, X. Dai⁶, E. Dall'Occo¹⁸, J. Dalseno⁴⁵, C. D'Ambrosio⁴⁷, J. Daniel¹¹,
A. Danilina⁴², P. d'Argent²², A. Davidson⁵⁵, J.E. Davies⁶¹, A. Davis⁶¹,
O. De Aguiar Francisco⁶¹, C. De Angelis^{30,j}, F. De Benedetti⁴⁷, J. de Boer³⁶,

G. Valenti²³ , N. Valls Canudas⁴⁷ , H. Van Hecke⁶⁶ , E. van Herwijnen⁶⁰ ,
C.B. Van Hulse^{45,w} , R. Van Laak⁴⁸ , M. van Veghel³⁶ , G. Vasquez⁴⁹ ,
R. Vazquez Gomez⁴⁴ , P. Vazquez Regueiro⁴⁵ , C. Vázquez Sierra⁴⁵ , S. Vecchi²⁴ ,
J.J. Velthuis⁵³ , M. Veltri^{25,v} , A. Venkateswaran⁴⁸ , M. Vesterinen⁵⁵ , D.
Vico Benet⁶² , P. V. Vidrier Villalba⁴⁴ , M. Vieites Diaz⁴⁷ , X. Vilasis-Cardona⁴³ ,
E. Vilella Figueras⁵⁹ , A. Villa²³ , P. Vincent¹⁵ , F.C. Volle⁵² , D. vom Bruch¹² ,
N. Voropaev⁴² , K. Vos⁷⁷ , G. Vouters^{10,47} , C. Vrahas⁵⁷ , J. Wagner¹⁸ , J. Walsh³³ ,
E.J. Walton^{1,55} , G. Wan⁶ , C. Wang²⁰ , G. Wang⁸ , J. Wang⁶ , J. Wang⁵ ,
J. Wang⁴ , J. Wang⁷² , M. Wang²⁸ , N. W. Wang⁷ , R. Wang⁵³ , X. Wang⁸,
X. Wang⁷⁰ , X. W. Wang⁶⁰ , Y. Wang⁶ , Z. Wang¹³ , Z. Wang⁴ , Z. Wang²⁸ ,
J.A. Ward^{55,1} , M. Waterlaet⁴⁷ , N.K. Watson⁵² , D. Websdale⁶⁰ , Y. Wei⁶ ,
J. Wendel⁷⁹ , B.D.C. Westhenry⁵³ , C. White⁵⁴ , M. Whitehead⁵⁸ , E. Whiter⁵² ,
A.R. Wiederhold⁵⁵ , D. Wiedner¹⁸ , G. Wilkinson⁶² , M.K. Wilkinson⁶⁴ ,
M. Williams⁶³ , M.R.J. Williams⁵⁷ , R. Williams⁵⁴ , Z. Williams⁵³ , F.F. Wilson⁵⁶ ,
W. Wislicki⁴⁰ , M. Witek³⁹ , L. Witola²⁰ , C.P. Wong⁶⁶ , G. Wormser¹³ ,
S.A. Wotton⁵⁴ , H. Wu⁶⁷ , J. Wu⁸ , Y. Wu⁶ , Z. Wu⁷ , K. Wyllie⁴⁷ , S. Xian⁷⁰,
Z. Xiang⁵ , Y. Xie⁸ , A. Xu³³ , J. Xu⁷ , L. Xu⁴ , L. Xu⁴ , M. Xu⁵⁵ , Z. Xu⁴⁷ ,
Z. Xu⁷ , Z. Xu⁵ , D. Yang , K. Yang⁶⁰ , S. Yang⁷ , X. Yang⁶ , Y. Yang^{27,l} ,
Z. Yang⁶ , Z. Yang⁶⁵ , V. Yeroshenko¹³ , H. Yeung⁶¹ , H. Yin⁸ , C. Y. Yu⁶ ,
J. Yu⁶⁹ , X. Yuan⁵ , Y. Yuan^{5,7} , E. Zaffaroni⁴⁸ , M. Zavertyaev¹⁹ , M. Zdybal³⁹ ,
F. Zenesini^{23,i} , C. Zeng^{5,7} , M. Zeng⁴ , C. Zhang⁶ , D. Zhang⁸ , J. Zhang⁷ ,
L. Zhang⁴ , S. Zhang⁶⁹ , S. Zhang⁶² , Y. Zhang⁶ , Y. Z. Zhang⁴ , Y. Zhao²⁰ ,
A. Zharkova⁴² , A. Zhelezov²⁰ , S. Z. Zheng⁶ , X. Z. Zheng⁴ , Y. Zheng⁷ ,
T. Zhou⁶ , X. Zhou⁸ , Y. Zhou⁷ , V. Zhovkovska⁵⁵ , L. Z. Zhu⁷ , X. Zhu⁴ ,
X. Zhu⁸ , V. Zhukov¹⁶ , J. Zhuo⁴⁶ , Q. Zou^{5,7} , D. Zuliani^{31,o} , G. Zunica⁴⁸ .

¹*School of Physics and Astronomy, Monash University, Melbourne, Australia*

²*Centro Brasileiro de Pesquisas Físicas (CBPF), Rio de Janeiro, Brazil*

³*Universidade Federal do Rio de Janeiro (UFRJ), Rio de Janeiro, Brazil*

⁴*Center for High Energy Physics, Tsinghua University, Beijing, China*

⁵*Institute Of High Energy Physics (IHEP), Beijing, China*

⁶*School of Physics State Key Laboratory of Nuclear Physics and Technology, Peking University, Beijing, China*

⁷*University of Chinese Academy of Sciences, Beijing, China*

⁸*Institute of Particle Physics, Central China Normal University, Wuhan, Hubei, China*

⁹*Consejo Nacional de Rectores (CONARE), San Jose, Costa Rica*

¹⁰*Université Savoie Mont Blanc, CNRS, IN2P3-LAPP, Annecy, France*

¹¹*Université Clermont Auvergne, CNRS/IN2P3, LPC, Clermont-Ferrand, France*

¹²*Aix Marseille Univ, CNRS/IN2P3, CPPM, Marseille, France*

¹³*Université Paris-Saclay, CNRS/IN2P3, IJCLab, Orsay, France*

¹⁴*Laboratoire Leprince-Ringuet, CNRS/IN2P3, Ecole Polytechnique, Institut Polytechnique de Paris, Palaiseau, France*

¹⁵*LPNHE, Sorbonne Université, Paris Diderot Sorbonne Paris Cité, CNRS/IN2P3, Paris, France*

¹⁶*I. Physikalisches Institut, RWTH Aachen University, Aachen, Germany*

¹⁷*Universität Bonn - Helmholtz-Institut für Strahlen und Kernphysik, Bonn, Germany*

¹⁸*Fakultät Physik, Technische Universität Dortmund, Dortmund, Germany*

¹⁹*Max-Planck-Institut für Kernphysik (MPIK), Heidelberg, Germany*

²⁰*Physikalisches Institut, Ruprecht-Karls-Universität Heidelberg, Heidelberg, Germany*

²¹*School of Physics, University College Dublin, Dublin, Ireland*

²²*INFN Sezione di Bari, Bari, Italy*

²³*INFN Sezione di Bologna, Bologna, Italy*

²⁴*INFN Sezione di Ferrara, Ferrara, Italy*

²⁵*INFN Sezione di Firenze, Firenze, Italy*

²⁶*INFN Laboratori Nazionali di Frascati, Frascati, Italy*

- ²⁷ INFN Sezione di Genova, Genova, Italy
- ²⁸ INFN Sezione di Milano, Milano, Italy
- ²⁹ INFN Sezione di Milano-Bicocca, Milano, Italy
- ³⁰ INFN Sezione di Cagliari, Monserrato, Italy
- ³¹ INFN Sezione di Padova, Padova, Italy
- ³² INFN Sezione di Perugia, Perugia, Italy
- ³³ INFN Sezione di Pisa, Pisa, Italy
- ³⁴ INFN Sezione di Roma La Sapienza, Roma, Italy
- ³⁵ INFN Sezione di Roma Tor Vergata, Roma, Italy
- ³⁶ Nikhef National Institute for Subatomic Physics, Amsterdam, Netherlands
- ³⁷ Nikhef National Institute for Subatomic Physics and VU University Amsterdam, Amsterdam, Netherlands
- ³⁸ AGH - University of Krakow, Faculty of Physics and Applied Computer Science, Kraków, Poland
- ³⁹ Henryk Niewodniczanski Institute of Nuclear Physics Polish Academy of Sciences, Kraków, Poland
- ⁴⁰ National Center for Nuclear Research (NCBJ), Warsaw, Poland
- ⁴¹ Horia Hulubei National Institute of Physics and Nuclear Engineering, Bucharest-Magurele, Romania
- ⁴² Affiliated with an institute covered by a cooperation agreement with CERN
- ⁴³ DS4DS, La Salle, Universitat Ramon Llull, Barcelona, Spain
- ⁴⁴ ICCUB, Universitat de Barcelona, Barcelona, Spain
- ⁴⁵ Instituto Galego de Física de Altas Enerxías (IGFAE), Universidade de Santiago de Compostela, Santiago de Compostela, Spain
- ⁴⁶ Instituto de Física Corpuscular, Centro Mixto Universidad de Valencia - CSIC, Valencia, Spain
- ⁴⁷ European Organization for Nuclear Research (CERN), Geneva, Switzerland
- ⁴⁸ Institute of Physics, Ecole Polytechnique Fédérale de Lausanne (EPFL), Lausanne, Switzerland
- ⁴⁹ Physik-Institut, Universität Zürich, Zürich, Switzerland
- ⁵⁰ NSC Kharkiv Institute of Physics and Technology (NSC KIPT), Kharkiv, Ukraine
- ⁵¹ Institute for Nuclear Research of the National Academy of Sciences (KINR), Kyiv, Ukraine
- ⁵² School of Physics and Astronomy, University of Birmingham, Birmingham, United Kingdom
- ⁵³ H.H. Wills Physics Laboratory, University of Bristol, Bristol, United Kingdom
- ⁵⁴ Cavendish Laboratory, University of Cambridge, Cambridge, United Kingdom
- ⁵⁵ Department of Physics, University of Warwick, Coventry, United Kingdom
- ⁵⁶ STFC Rutherford Appleton Laboratory, Didcot, United Kingdom
- ⁵⁷ School of Physics and Astronomy, University of Edinburgh, Edinburgh, United Kingdom
- ⁵⁸ School of Physics and Astronomy, University of Glasgow, Glasgow, United Kingdom
- ⁵⁹ Oliver Lodge Laboratory, University of Liverpool, Liverpool, United Kingdom
- ⁶⁰ Imperial College London, London, United Kingdom
- ⁶¹ Department of Physics and Astronomy, University of Manchester, Manchester, United Kingdom
- ⁶² Department of Physics, University of Oxford, Oxford, United Kingdom
- ⁶³ Massachusetts Institute of Technology, Cambridge, MA, United States
- ⁶⁴ University of Cincinnati, Cincinnati, OH, United States
- ⁶⁵ University of Maryland, College Park, MD, United States
- ⁶⁶ Los Alamos National Laboratory (LANL), Los Alamos, NM, United States
- ⁶⁷ Syracuse University, Syracuse, NY, United States
- ⁶⁸ Pontifícia Universidade Católica do Rio de Janeiro (PUC-Rio), Rio de Janeiro, Brazil, associated to ³
- ⁶⁹ School of Physics and Electronics, Hunan University, Changsha City, China, associated to ⁸
- ⁷⁰ Guangdong Provincial Key Laboratory of Nuclear Science, Guangdong-Hong Kong Joint Laboratory of Quantum Matter, Institute of Quantum Matter, South China Normal University, Guangzhou, China, associated to ⁴
- ⁷¹ Lanzhou University, Lanzhou, China, associated to ⁵
- ⁷² School of Physics and Technology, Wuhan University, Wuhan, China, associated to ⁴
- ⁷³ Departamento de Física, Universidad Nacional de Colombia, Bogota, Colombia, associated to ¹⁵
- ⁷⁴ Ruhr Universitaet Bochum, Fakultae f. Physik und Astronomie, Bochum, Germany, associated to ¹⁸
- ⁷⁵ Eotvos Lorand University, Budapest, Hungary, associated to ⁴⁷
- ⁷⁶ Van Swinderen Institute, University of Groningen, Groningen, Netherlands, associated to ³⁶
- ⁷⁷ Universiteit Maastricht, Maastricht, Netherlands, associated to ³⁶
- ⁷⁸ Tadeusz Kosciuszko Cracow University of Technology, Cracow, Poland, associated to ³⁹

- ⁷⁹ *Universidade da Coruña, A Coruna, Spain, associated to* ⁴³
- ⁸⁰ *Department of Physics and Astronomy, Uppsala University, Uppsala, Sweden, associated to* ⁵⁸
- ⁸¹ *University of Michigan, Ann Arbor, MI, United States, associated to* ⁶⁷
- ⁸² *Département de Physique Nucléaire (DPhN), Gif-Sur-Yvette, France*
- ^a *Universidade de Brasília, Brasília, Brazil*
- ^b *Centro Federal de Educação Tecnológica Celso Suckow da Fonseca, Rio De Janeiro, Brazil*
- ^c *Hangzhou Institute for Advanced Study, UCAS, Hangzhou, China*
- ^d *School of Physics and Electronics, Henan University, Kaifeng, China*
- ^e *LIP6, Sorbonne Université, Paris, France*
- ^f *Universidad Nacional Autónoma de Honduras, Tegucigalpa, Honduras*
- ^g *Università di Bari, Bari, Italy*
- ^h *Università di Bergamo, Bergamo, Italy*
- ⁱ *Università di Bologna, Bologna, Italy*
- ^j *Università di Cagliari, Cagliari, Italy*
- ^k *Università di Ferrara, Ferrara, Italy*
- ^l *Università di Genova, Genova, Italy*
- ^m *Università degli Studi di Milano, Milano, Italy*
- ⁿ *Università degli Studi di Milano-Bicocca, Milano, Italy*
- ^o *Università di Padova, Padova, Italy*
- ^p *Università di Perugia, Perugia, Italy*
- ^q *Scuola Normale Superiore, Pisa, Italy*
- ^r *Università di Pisa, Pisa, Italy*
- ^s *Università della Basilicata, Potenza, Italy*
- ^t *Università di Roma Tor Vergata, Roma, Italy*
- ^u *Università di Siena, Siena, Italy*
- ^v *Università di Urbino, Urbino, Italy*
- ^w *Universidad de Alcalá, Alcalá de Henares, Spain*
- ^x *Facultad de Ciencias Físicas, Madrid, Spain*
- ^y *Department of Physics/Division of Particle Physics, Lund, Sweden*
- [†] *Deceased*